PRODUCTION OF LIGHT NUCLEI IN FISSION OF URANIUM ISOTOPES INDUCED BY THERMAL NEUTRONS

A. A. Vorob'ev, V. T. Grachev,
I. A. Kondurov, A. M. Nikitin,
and D. M. Selivestrov

The results of an experimental study of the light nuclei produced in ternary fission of uranium isotopes induced by thermal neutrons are reported. The experimental procedure is described. Data are given on the yields and energy spectra of hydrogen, helium, lithium, and beryllium isotopes. The results are compared with theoretical data and with experimental data obtained during fission induced by fast protons.

INTRODUCTION

The experimental data available are consistent with the assertion that ternary fission proceeds in the same way as binary fission at all stages up to the instant at which the neck to the parent nucleus ruptures [1]. This conclusion is reached on the basis of a study of fission accompanied by α emission (α fission). It has been shown [2, 3] that the mass distributions of the fragments produced in binary fission are similar to those produced in α fission. It was later shown that the probability for α fission, like the kinetic energy of the fragments in binary fission, does not depend on the excitation energy of the parent nucleus [4]. Both quantities are apparently governed by the nuclear configuration at the time of fission, and this configuration does not depend on the excitation energy. Finally, a parallel can be drawn between the dependence of the angular distribution of α's on the mass ratio of the fragments and the analogous dependence of the average number of neutrons emitted by fragments in binary fission [5].

Accordingly, studies of binary and ternary fission amount to studies of different exit channels of the same process. Obviously, three particles carry much more information about the final stage of fission than do two particles, so progress can hopefully be achieved in understanding the behavior of the parent nucleus after passage through the saddle point. In particular, construction of a theory of fission requires information about the kinetic energy of the fragment at the instant of neck rupture. If, e.g., it is established that this energy is much greater than 1 MeV, the statistical approach to fission theory would have to be abandoned [6], for it requires the establishment of thermodynamic equilibrium immediately before the rupture.

However, it is not a simple problem to extract information about a nucleus undergoing fission from the observed characteristics of ternary fission. Many attempts have been made [7-12] to determine the initial energies of the three fragments (i.e., the energies at the instant of rupture) from the observed final angular and energy distributions, without resorting to any specific model for the α production, using only the assumption that the α is produced in the space between the two fragments at the instant the neck ruptures. In this determination, the initial distributions of coordinates and velocities of the particles are first specified with a small number of free parameters (e.g., the average energy of the heavy fragments and the average α energy). Then the problem of the separation of three bodies under the influence of a Coulomb repulsive force is solved, and the free parameters are selected for optimum agreement between the calculated and experimental angular and energy distributions of the final particles. Unfortunately,

A. F. Ioffe Physicotechnical Institute. Translated from Problemy Fiziki Élementarnykh Chastits i Atomnogo Yadra, Vol. 2, No. 4, pp. 939-958, 1972.

TABLE 1. Basic Parameters of the Magnetic Time-of-Flight Mass Spectrometer

Parameter	Value	Note
Energy resolution $\Delta E/E$	0,7%	For ^{244}Cm α's E_α = 5.806 MeV
Time resolution $\Delta T/T$	0,5%	For ^{244}Cm α's T_α = 360 nsec
Resolution of magnetic analyzer $\Delta B_\varphi/B_\varphi$	2,5—5%	With a target diameter of 5-10 mm and a detector diameter of 10 mm
Mass resolution $\Delta M/M$	1%	With an account of the resolution of the magnetic analyzer
Solid angle Ω	$1 \cdot 10^{-4}$ sr	With collimators to shut off direct paths from the reactor zone
Energy threshold of detection E_{min}	2 MeV 4—5 MeV	For H and He isotopes For Li and Be isotopes

agreement with the experimental data can be achieved with different sets of initial conditions, although it is true that at present a detailed comparison has been carried out primarily for the process which has received the most study – fision involving α emission. The situation could be improved by new experimental data, particularly on fission involving the production of other light nuclei.

Fission involving the production of light nuclei is also of independent interest, since the light nuclei are produced under very unusual conditions of maximum nuclear deformation – conditions not found in other nuclear reactions. With the appearance of new methods for identifying particles there has been a sharp increase in the capabilities of ternary-fission studies. It has been shown that α's are not the only products of fission: other helium and hydrogen isotopes, as well as isotopes of lithium, beryllium, and heavier elements, are also produced [13-16]. It was shown in [11] that the angular distributions of ^{3}H, ^{6}He, and lithium and beryllium nuclei are similar to the angular distribution of α's. This result implies that all the light nuclei are produced in ternary fission as α's are.

Below we report a study of the isotopic composition and energy spectra of light nuclei produced during the fission of ^{235}U and ^{233}U induced by thermal neutrons.

Experimental Procedure

In most of the experiments the particles were identified by ΔE-E telescopes of semiconductor detectors. Using this method, one can distinguish between hydrogen and helium isotopes, but the mass resolution is not adequate for isotopic separation of lithium, beryllium, or the heavier elements produced in low-energy fission. Moreover, because of the thick entrance window of the telescopes, only the high-energy part of the spectrum can be measured. A mass spectrometer was used which simultaneously measured the following particle properties: $B\rho$, v, E, $\Delta E/\Delta x$. A mass spectrometer has the advantages of a better mass resolution and a thinner entrance window over a telescope.

An important part of the spectrometer is the magnetic analyzer with double focusing, which consists of four quadropole lenses (Q1 and Q2, Fig. 1). The lenses provide two focal planes, 6 and 12 m from the target, which is in a reactor-neutron flux of 10^{13} cm^{-2} · sec^{-1}. The particle energy is measured by a Si(Au) detector in the second focal plane. The fast signal from this detector is used as a stop signal for the time-amplitude converter. The start signal is produced in the following manner: In the first focal plane there is an Al foil 0.15 mg-wt/cm^2 thick; secondary electrons which are produced during the passage of particles through the foil and which are then accelerated to 20 keV are detected by two scintillation counters in a coincidence circuit. In some of the experiments, a ΔE detector was placed in front of the E de-

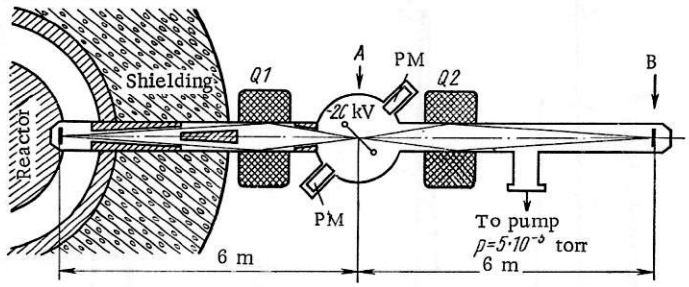

Fig. 1. Spectrometer layout.

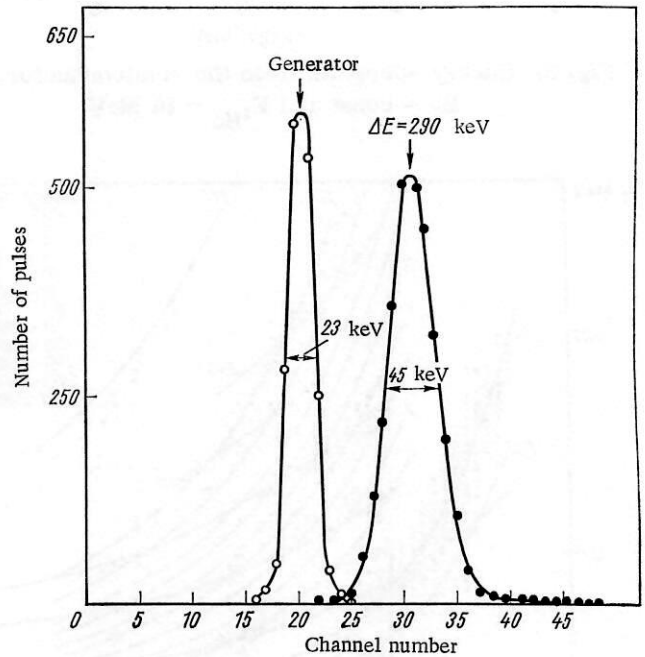

Fig. 2. Pulse spectrum from the ΔE detector corresponding to ^{244}Cm α's. The gas pressure is 50 torr.

tector and used as a planar ionization chamber with a grid. Particles were brought in to the chamber parallel to the electrodes. The sensitive layer of the chamber is 50 mm thick. The chamber is filled with a mixture of argon and methane (99% Ar + 1% CH_4) at a pressure of 40-100 torr. The chamber is separated from the rest of the evacuated part of the spectrometer by a colloidal film equivalent in terms of absorption to 0.35 mg-wt/cm^2 of Al. Figure 2 shows the energy resolution of the ΔE detector. The basic parameters of the mass spectrometer are shown in Table 1; the E_{min} values shown here are governed largely by scattering and charge exchange of charged particles in the aluminum foil at the first focal point of the magnetic analyzer (discussed in more detail below). The α count rate at the peak of the energy distribution is $n_\alpha = 15$ sec^{-1} with a target consisting of 0.6 mg-wt of $^{233}U_3O_8$. Targets ranging in thickness from 0.09 to 4 mg-wt/cm^2 were used in various experiments; in some of the experiments the targets were covered with Al foil 4.1 mg-wt/cm^2 thick for total absorption of the fission fragments. The measurements were carried out under various conditions; in the two-parameter regime the energy spectrum from the E detector was measured with $B\rho$ = const (Fig. 3). Only the isotopes ^{4}He, ^{6}He, ^{3}H, ^{2}H, and ^{1}H could be separated in this regime. The two-parameter analysis can be carried out in three versions: E-T, E-ΔE, T-ΔE. Figure 4 shows the T-E spectrum obtained in the absence of the ΔE detector. In the T-E-ΔE three-parameter analysis, all the information for a fixed value of $B\rho$ is recorded on magnetic tape; then a computer prints out any desired two-dimensional spectrum for a given value of the third parameter. Figure 5 shows such a T-ΔE spectrum. Since the mass resolution is governed by the accuracy of the E and T mea-

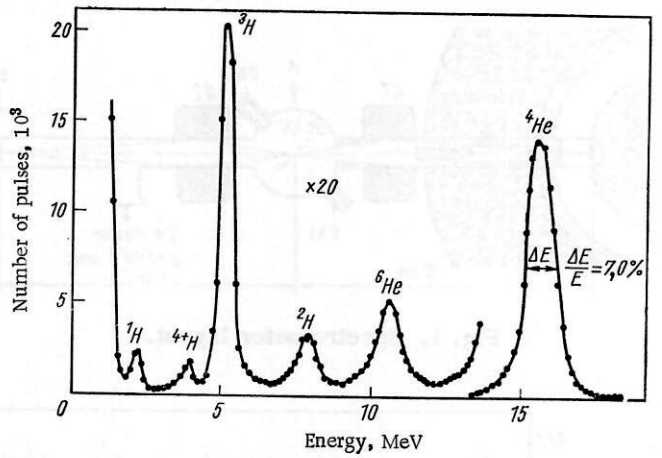

Fig. 3. Energy spectrum from the semiconductor, for $B\rho$ = const and $E_{^4He}$ = 16 MeV.

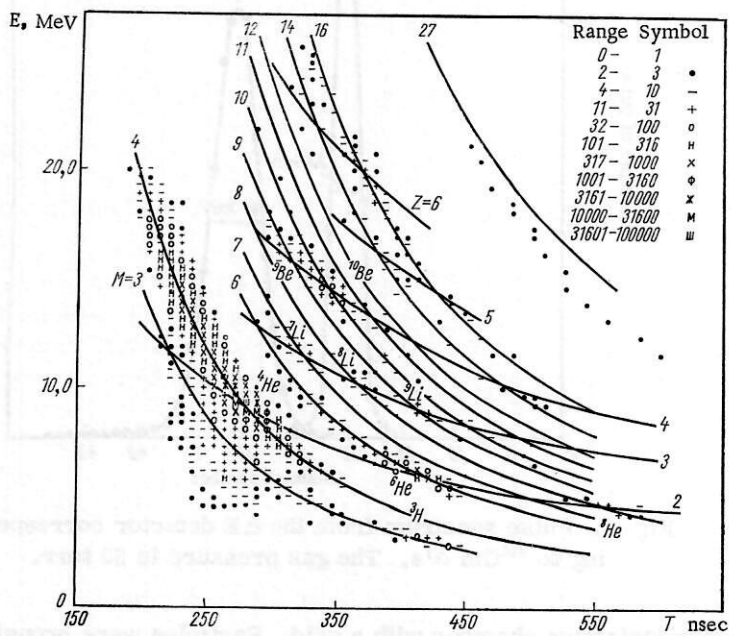

Fig. 4. Two-parameter E-T spectrum, for $B\rho$ = const and $E_{^4He}$ = 9 MeV. The solid curves show the calculated energies and flight times for particles having the given mass and charge.

surements, while $\Delta E/\Delta x$ is measured only to identify the charge of the particle, the mass spectrum of particles detected is ultimately governed by the E-T measurements.

The spectrometer was calibrated on the basis of ^3H and ^4He nuclei from the $^6Li(n, \alpha)^3H$ reaction ($E_{^3H}$ = 2.73 MeV, E_α = 2.05 MeV) and ^{244}Cm α's (E_α = 5.806 MeV). Control experiments showed the solid angle of the spectrometer to remain constant over the entire $B\rho$ range measured. Figure 6 shows the α spectra measured by various methods for the case of ^{235}U fission induced by thermal neutrons. Comparison shows that measurements with the magnetic time-of-flight mass spectrometer do not involve any systematic errors.

In a measurement of the spectra of multicharged particles, certain corrections must be introduced; we studied this subject in detail. The isotope yield is found as a ratio with respect to the α yield:

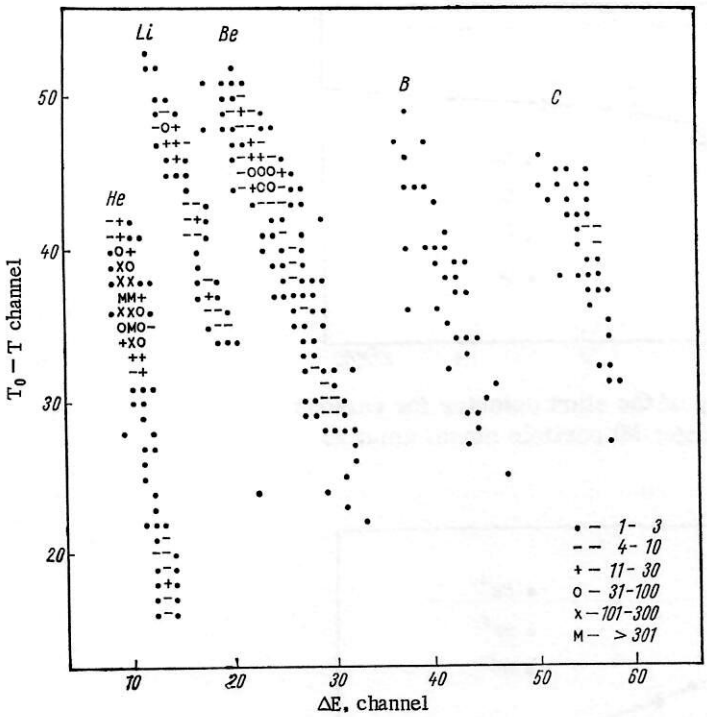

Fig. 5

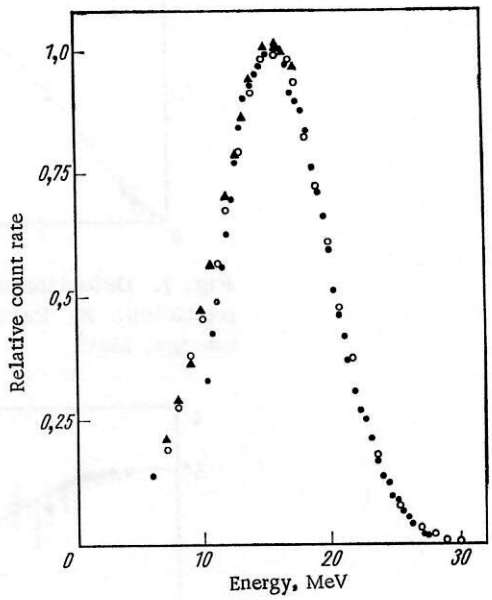

Fig. 6

Fig. 5. Two-parameter T-ΔE spectrum (Bρ = const, $E_{^4He}$ = 8 MeV, and 50 torr; T_0 is the measured interval).

Fig. 6. Comparison of the energy spectra of ^{4}He nuclei produced in ^{235}U fission induced by thermal neutrons. The measurements were carried out by various methods. Filled circles) Data of this study, obtained with a magnetic analyzer; triangles) data of [18], obtained by the ΔE method with a gas-filled proportional counter as ΔE detector; filled circles) data of [14] obtained by the ΔE method with a 50-μ semiconductor as ΔE detector.

$$\frac{Y_x}{Y_\alpha} = \frac{N_x}{N_\alpha} \cdot \frac{1}{K_x} \cdot \frac{\varepsilon_\alpha}{\varepsilon_x},$$

where Y_X is the yield of isotope x per 1-MeV energy interval with Bρ = const, N_X is the number of particles detected, and K_X is a factor which takes into account the variations in the energy intervals singled out by the magnetic spectrometer:

$$K_x = \frac{M_\alpha}{M_x}\left(\frac{Z_x}{Z_\alpha}\right)^2;$$

where ε_X is the efficiency with which isotope x is detected. This efficiency is governed primarily by three factors:

$$\varepsilon_x = \varepsilon_x^0 \varepsilon_x^c \varepsilon_x^i.$$

where ε_X^0 is the efficiency of the start detector. Comparison of the results found in the one-parameter (E) and two-parameter (E-T) analyses show that ε_X^0 is a function of the parameter Z^2M/E, which determines the specific ionization $\Delta E/\Delta x$. Figure 7 shows the dependence of ε_X^0 on Z^2M/E. The factor ε_X^c takes into account the reduction in count rate due to Coulomb scattering of particles in the start detector; the factor ε_X^c, a function of Z/E, was determined experimentally in a one-parameter analysis using the particles ^{4}He, ^{6}He, and ^{3}H (Fig. 8). The corrections due to ε_X^0 and ε_X^c were usually small and could be reliably determined experimentally, so the uncertainties arising from the use of these corrections do not exceed a few percent. The factor ε_X^i is due to the charge distribution of particles emitted from the target and to the change in the

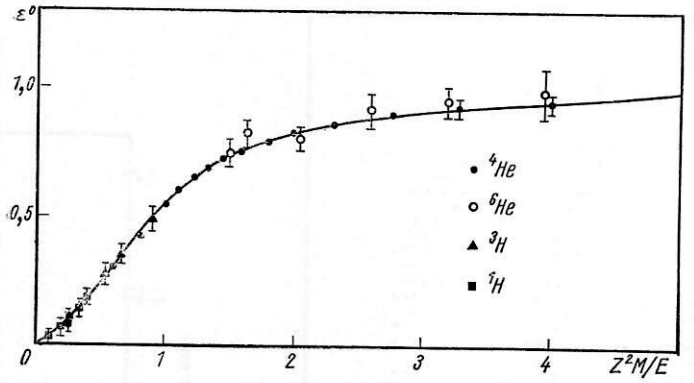

Fig. 7. Detection efficiency of the start detector for various particles. Z) Particle charge; M) particle mass, amu; E) energy, MeV.

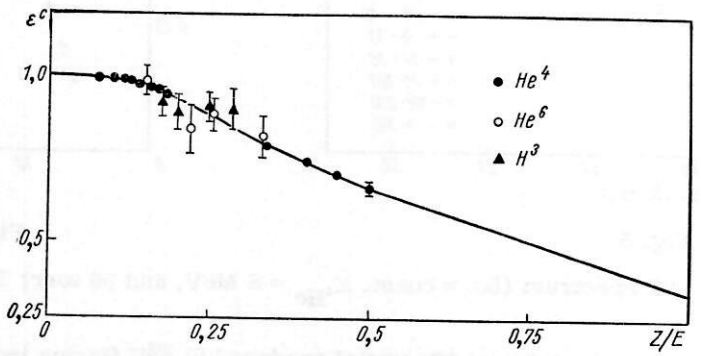

Fig. 8. Correction for scattering in the start detector for various particles.

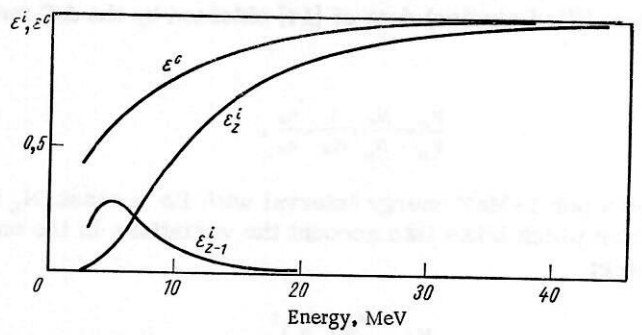

Fig. 9. Effect of scattering and charge exchange of ^{10}Be nuclei on the detection efficiency.

particle charge during passage through the start detector; it satisfies $\varepsilon^i_x = (\Phi^i_x)^2$, where Φ^i_x is the probability that a particle x(Z, M) will have a charge i after passage through the aluminum foil. The values of Φ^i_x are from [19]. The validity of introducing a correction for ion charge exchange was checked by determining the yields of ^{10}Be in the range 6-10 MeV through the detection of $^{10}Be^{+4}$ and $^{10}Be^{+3}$ ions; the results agreed within 10%. Figure 9 shows all the correction coefficients for the determination of the ^{10}Be yield.

A study was made of the dependence of the count rate of ^3H, $^4He^{++}$, and $^4He^+$ ions on the residual gas pressure in the vacuum chamber of the spectrometer (Fig. 10); the observed decrease in the count rate is due to scattering of particles in the case of ^3H and $^4He^{++}$, and it is due to charge exchange in the case of $^4He^+$. A pressure of $3 \cdot 10^{-5}$ torr turned out to be low enough to eliminate the effect of atomic collisions in the gas on the detection efficiency of the spectrometer. This conclusion was also checked in measurement of the yields of ^7Li and ^{10}Be nuclei during fission.

TABLE 2. Most Probable Energies of Particles Produced in the Fission of Various Nuclei, MeV

Particle	^{234}U [20]	^{236}U (this study)	^{238}U [14]	^{240}Pu [21]	^{252}Cf [13]
^{1}H	—	—	8,6±0,3	8,4±0,15	7,8±0,8
^{2}H	8,4±0,15	8,6±0,15	7,9±0,3	8,2±0,3	8,0±0,5
^{3}H	8,4±0,15	8,2±0,1	8,6±0,3	8,2±0,15	8,0±0,3
^{4}He	16,3±0,1	15,9±0,1	15,7±0,3	16,0±0,1	16,0±0,2
^{6}He	11,5±0,2	11,1±0,2	12,0±0,5	11,8±0,4	12,0±0,5
^{8}He	9,7±0,25	10,2±0,2	—	<12,0	10,2±1,0
^{7}Li	15,8±0,25	14,8±0,9	—	—	—
^{8}Li	14,4±0,5	13,2±0,9	—	—	—
^{10}Be	17,0±0,4	17,5±0,6	—	—	—

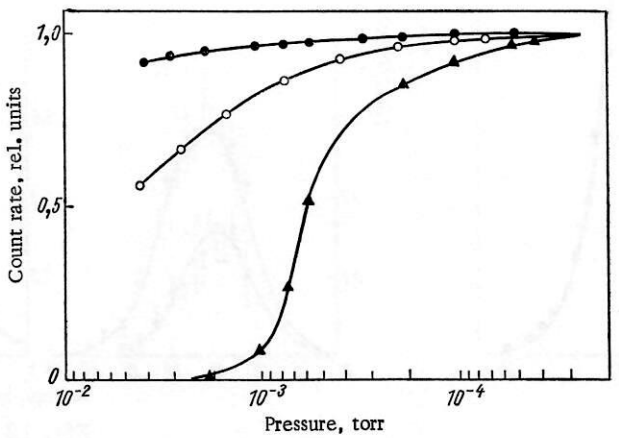

Fig. 10. Dependence of the count rate of the products of the ^{6}Li(n, ^{3}H)^{4}He reaction on the residual gas pressure in the vacuum chamber of the spectrometer.

Experimental Results

Figures 11 and 12 show the energy spectra of ^{2}H, ^{3}H, ^{4}He, ^{6}He, ^{7}Li, ^{8}Li, and ^{10}Be isotopes formed during the fission of ^{234}U after the capture of neutrons by ^{233}U. The solid curves show the approximations of the experimental data by normal distributions. The proton spectrum was not obtained because of the uncertainty regarding the subtraction of the background due to the (n, p) reaction in the target substrate, which is extremely important for protons having energies up to 10 MeV. There is also some contribution to the ^{4}He spectrum from (n, α) reactions (Fig. 11). The background contributions are insignificant for the other isotopes. The energy spectra of the light nuclei produced during the fission of ^{236}U are similar to the spectra shown in Figs. 11 and 12. Tables 2 and 3 show the parameters used to approximate the experimental results by normal distributions (the most probable energy E_{max} and the full width at half maximum fwhm). Shown here for comparison are data obtained by other investigators for the low-energy fission of ^{236}U, ^{240}Pu, and ^{252}Cf. All the errors indicated for E_{max} and the fwhm are statistical errors; only for the ^{4}He spectra (measured with the magnetic time-of-flight mass spectrometer) are the errors in E_{max} and the fwhm governed primarily by the calibration accuracy of the spectrometer, ±100 keV. Table 4 shows the extrapolated yields of various light nuclei. The extrapolated yields are found as the areas under the Gaussian curves and are normalized in terms of the extrapolated yield for ^{4}He. The ^{3}He yield turned out to be very low; a special series of experiments with an improved analyzer line shape was carried out to determine it. The line shape of the focusing systems, which consist of quadropole lenses, has a high-energy tail, which hinders resolution of the weak ^{3}He line against the background of the intense ^{4}He line (Fig. 4). A target 6 mm in diameter and a special differentiation were used to reduce this tail, and a high count rate was achieved with a $^{235}U_3O_8$ target 6 mg-wt./cm^2 in thickness. These measures reduced the tail by a factor of several tens. More than 10^6 α's were recorded, but the upper limit on the ^{3}He-production probability could not be established. For the case of the ^{6}Li yield, the T-E-ΔE method is used

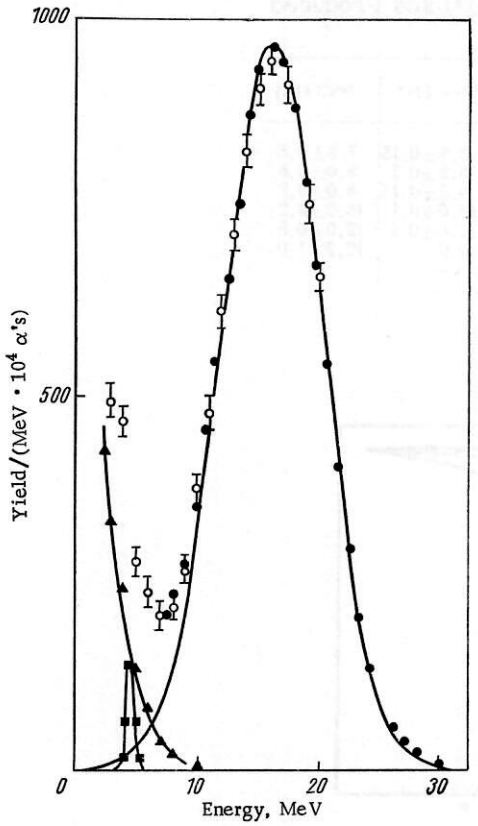

Fig. 11

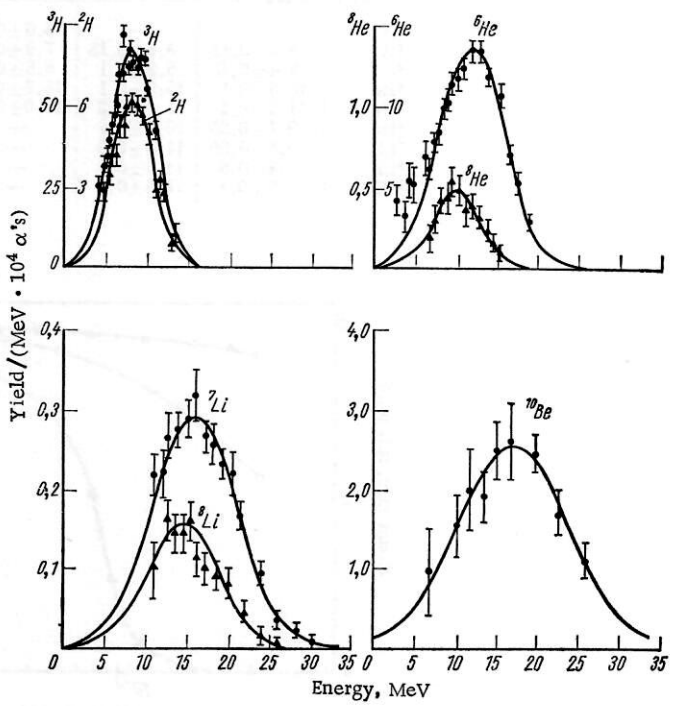

Fig. 12

Fig. 11. Energy spectrum of ^{4}He nuclei produced in the fission of ^{233}U by neutrons. Filled circles) U_3O_8 target 1.2 mg-wt./cm^2 thick covered with a foil 4.1 mg-wt./cm^2 thick. The spectrum is corrected for the absorption of the α energy in the target and in the Al foil; open circles) target 0.09 mg-wt./cm^2 thick and Al foil 0.15 mg-wt./cm^2 thick. The spectrum was obtained without subtraction of background; triangles) background from the (n, α) reaction, normalized in terms of the ^{4}He spectrum obtained with a target 0.09 mg-wt./ cm^2 thick; squares) spectrum of natural α background, found in the absence of the neutron flux.

Fig. 12. Energy spectra of hydrogen, helium, lithium, and beryllium isotopes produced in the fission of ^{233}U by neutrons. The ^{10}Be spectrum and the part of the ^{6}He spectrum below 7 MeV were measured with a target 0.09 mg-wt./cm^2 thick covered by Al foil 0.15 mg-wt./cm^2 thick. The other spectra were obtained with a U_3O_8 target 1.2 mg-wt./cm^2 thick and Al foil 4.1 mg-wt./cm^2 thick. The spectra are corrected for absorption of the particle energy in the target and in the Al foil.

with a single value of Bρ corresponding to the energy of the ^{6}Li nuclei produced in the target: 17 MeV. Six ^{6}Li nuclei were detected per 430 ^{7}Li nuclei. A peak in the expected ^{6}Li energy spectrum occurs at 16-18 MeV.

The yields of all the isotopes were measured with respect to the α yield. To determine the absolute yield (more precisely, the yield with respect to the number of binary fission events), we can use the probability for α emission per fission α/F, found from other experiments. Knowledge of the absolute yields for the various isotopes is important in a comparative study of the ternary fission of various heavy nuclei. On the other hand, the value of α/F can be determined on the basis of these results and data on the radiochemical yield of tritium for the fission of ^{233}U and ^{235}U by thermal neutrons: $F/{}^3H = (1.05 \pm 0.09) \cdot 10^4$ (^{235}U) [24] and $F^3/H = (1.10 \pm 0.07) \cdot 10^4$ (^{233}U) [25]. Using these data on the tritium yield $^3H/\alpha$, we can determine F/α: $F/\alpha = 760 \pm 80$ (^{235}U) and $F/\alpha = 510 \pm 35$ (^{233}U).

TABLE 3. Widths of the Energy Distributions of Particles Produced during the Fission of Various Nuclei (MeV)

Particle	^{234}U [20]	^{236}U (this study)	^{236}U [14]	^{240}Pu [21]	^{252}Cf [13]
^{1}H	—	—	6,9±0,5	7,2±0,3	6,8±1,6
^{2}H	6,3±0,3	7,1±0,2	7,0±1,0	7,2±0,5	7,2±1,0
^{3}H	6,5±0,3	6,5±0,2	6,7±0,6	7,6±0,4	6,2±0,6
^{4}He	9,7±0,15	9,8±0,1	9,8±0,4	10,6±0,2	10,2±0,4
^{6}He	9,5±0,3	11,2±0,2	8,7±0,7	10,6±0,6	8,0±1,0
^{8}He	6,9±0,5	6,8±0,4	—	>9,0	8,0±2,0
^{7}Li	12,1±0,4	13,0±1,0	—	—	—
^{8}Li	10,6±0,8	12,1±1,3	—	—	—
^{10}Be	15,7±0,9	15,2±0,9	—	—	—

TABLE 4. Extrapolated Yields of Particles Produced during Fission

Particle	^{234}U [20]	^{236}U (this study)	^{236}U [14, 22]	^{240}Pu [21]	^{240}Pu [23]	^{252}Cf [13]
^{1}H	—	—	115±15	190±10	—	175±30
^{2}H	41±2	50±2	50±10	50±10	—	68±3
^{3}H	460±20	720±30	630±50	680±30	—	846±28
^{3}He	—	≤0,01	—	—	—	—
^{5}He	10^{4}	10^{4}	10^{9}	10^{4}	10^{4}	10^{4}
^{6}He	137±6	198±8	>110	190±20	250	263±18
^{8}He	3,6±0,4	6,0±0,4	—	8,0±2,0	—	9,0±1,2
^{6}Li	≤0,05	≤0,05	—	—	—	—
^{7}Li	3,7±0,2	4,4±0,6	—	—	—	—
^{8}Li	1,8±0,2	2,6±0,3	—	—	—	—
^{9}Li	3,6±0,5	3,8±1,0	—	—	—	—
ΣLi	9,1	10,8	12±2	—	15	13,2±1,0
^{7}Be	≤0,01	≤0,01	—	—	—	—
^{9}Be	3,7±0,8	3,2±0,5	—	—	—	—
^{10}Be	43±3	37±3	—	—	—	—
^{11}Be	—	≤1,4	—	—	—	—
ΣBe	46,7	40,2	37±4	—	58,5	20,1±2,0

In a special series of experiments, an attempt was made to detect the isotope ^{10}He among the products of the ^{235}U fission induced by thermal neutrons [26]. Since no theory is available to explain the probability for the production of light nuclei in fission, our only method for predicting the ^{10}He yield was to extrapolate the yields of ^{4}He, ^{6}He, and ^{8}He. This extrapolation leads to a ^{10}He count rate approximately 0.02 of the ^{8}He count rate. In the T-E-Δ regime, 2500 ^{8}He nuclei were detected, but not a single event which could be identified as the emission of a ^{10}He nucleus was detected. This result seems to be evidence against the existence of the unstable isotope ^{10}He (for a more detailed discussion, see [26]).

Discussion of Results

As Tables 2-4 show, the energy spectra of the light particles are essentially independent of Z^2/A of the parent nucleus; this fact requires an explanation, particularly since the maximum observed discrepancy in the ^{4}He spectra corresponds to the fission of the two neighboring nuclei ^{234}U and ^{236}U. The yields of light nuclei produced during the fission of ^{234}U and ^{236}U also display differences, and the yield increases with increase of Z^2/A of the parent nucleus.

Interestingly, the yield of neutron-deficient isotopes (^{3}He, ^{6}Li, and ^{7}Be) is low. At present, no satisfactory explanation has been advanced for this effect, so it is interesting to compare the relative yields of the light nuclei in ternary fission with the yields of the same nuclei produced during bombardment of ^{238}U by 5.5-GeV protons [27] (Table 5). We see that in the latter case the ^{3}He, ^{6}Li, and ^{7}Be yields are quite large. This comparison would seem to furnish a basis for treating the low-energy fission as "anomalous" (in the sense that neutron-deficient nuclei are produced), so an explanation should be sought for this anomaly in, e.g., neutron enrichment of the neck of the parent nucleus. However, this conclusion would be premature: Experimental data [26] show that the energy spectra and angular distributions of the neutron-deficient nuclei produced during the bombardment of ^{238}U by 5.5 GeV protons differ markedly from analogous characteristics of the other isotopes. The yield in the direction of the incident beam is increased, and the

TABLE 5. Comparison of the Yields of Certain Light Nuclei Produced in Various Reactions

Production method	^{3}He	^{4}He	^{6}He	^{8}He	^{6}Li	^{7}Li	^{8}Li	^{9}Li	^{7}Be	^{9}Be	^{10}Be	^{11}Be
^{236}U fission (this study)	$\leqslant$0,01	10^4	198	6,0	$\leqslant$0,05	4,4	2,6	3,8	$\leqslant$0,01	3,2	37	$\leqslant$1,4
^{238}U + P [27], E_p = 5.5 GeV	1600	10^4	234	11,3	196	440	132	40	47	130	147	13

Note. All yields are expressed per 10^4 α's.

TABLE 6. Probabilities for the Production of Light Nuclei in ^{236}U Fission

Particle	Particle production energy E_{RX}, MeV, acc. to Halpern*	Observed yield per fission†	No. of fission events in which the deformation energy is sufficient for production of the light nucleus
^{3}H	25	$0{,}95\cdot10^{-4}$	$3\cdot10^{-3}$
^{4}He	27	$1{,}3\cdot10^{-3}$	$1{,}5\cdot10^{-3}$
^{6}He	33	$2{,}6\cdot10^{-5}$	$1\cdot10^{-4}$
^{8}He	44	$0{,}8\cdot10^{-6}$	10^{-6}
^{7}Li	48	$6\cdot10^{-7}$	10^{-7}
^{9}Li	53	$5\cdot10^{-7}$	$<10^{-8}$
^{10}Be	55	$4{,}5\cdot10^{-6}$	$<10^{-9}$

* The E_{RX} values were determined for the case in which the particles were produced from the heavy fragment.
† In the determination of the particle yields per fission, use was made of the probability for tritium production per fission event: $^{3}H/F = (0.95 \pm 0.09) \cdot 10^{-4}$ [24].

energy spectra fall off more smoothly as a function of the energy. In this case also neutron-deficient nuclei are apparently produced only when an anomalously large excitation energy (and momentum) remains as a result of the development of a cascade; alternately, it may be that nuclei such as ^{3}He are produced in an inelastic interaction of cascade protons with "primary" and heavier clusters (in this case, ^{4}He).

The accumulation of data on the production probabilities for light nuclei in ternary fission opens up new possibilities for checking ternary-fission models. The production of a light nucleus involves the expenditure of a certain amount of energy, so the primary task of a ternary-fission model is to indicate the source of this energy. According to the Halpern model [28], light nuclei are produced by means of energy involved in the deformation of the parent nucleus. The magnitude of this energy is assumed equal to the excitation energy E^*_{bf} of the binary-fission fragments. In turn, E^*_{bf} is determined by comparing the kinetic energy of the fragments with the mass defect and from experiments in which the number of neutrons emitted by the fragments are measured. Experiment shows that E^*_{bf} can be approximated by a Gaussian distribution, with distribution parameters which turn out to depend on the mass ratio of the fragments. According to [29], in the fission of ^{235}U induced by thermal neutrons, $E^*_{bf} \pm \sigma(E^*_{bf})$ for the most probable mass ratio is 24 $\pm$ 8.5 MeV. Halpern estimated the energy required for the production of light nucleus X in the following manner: The two fragments L and H, in their ground states, are separated by a distance in which the potential energy of the fragments is equal to the total kinetic energy. Then the work E_{RX} which must be performed to separate light nucleus X from one of the fragments and to place this nucleus between the fragments on the line connecting their centers is calculated. Then the kinetic energy K_X of the light particle must be added to E_{RX}, along with the deformation-excitation energy E^*_{te} of the fragments, in ternary fission. The value of $E_X = E_{RX} + K_X + E^*_{te}$ obtained in this manner can be compared with the energy E^*_{bf}; calculated values of E_{RX} are shown in Table 6. The value of K_X is usually small (1-3 MeV), and for rough estimates it can be assumed to have the same value, e.g., K_X = 2 MeV, for all nuclei. The value of E^*_{te} is determined only for the case of fission involving α emission. It turns out that the excitation energy of fragments in the case of ternary fission is only slightly less than the excitation

energy of the fragments in binary fission: the difference is 6 ± 2 MeV [30]. It was shown in [31] that the number of neutrons in fission events involving the emission of ^{4}He, ^{3}H, and ^{1}H is essentially the same. No information is available on the value of E^*_{te} for fission involving the emission of the particles. It might be assumed that this energy is approximately equal to $E^*_{te} \approx 20$ MeV in all cases. Now adopting as the E^*_{bf} distribution a Gaussian distribution with the parameters given above, we can calculate the probability that the deformation energy of the fragments exceeds E_X during binary fission. Table 6 yields the probabilities determined in this manner. Comparison with the observed yields implies that the deformation energy of the fragments produced in fission is not adequate for the production of light nuclei having $Z \geq 4$. Further evidence for the assertion that the deformation-excitation energy does not alone govern the probability for ternary fission is the fact that no significant increase in the probability for ternary fission [3] is observed for symmetric fission. However, if the deformation energy of the fragments is not sufficient for the production of light nuclei, we must assume that the fragments acquire a quite large kinetic energy (30-40 MeV) at the instant of rupture and that light nuclei are produced primarily at the expense of this energy. Under this assumption the fragments produced in binary fission should have their maximum kinetic energy immediately after rupture, and the magnitude of this energy should fall off with increasing E_X. The observed energy and angular distributions of the particles produced in ternary fission are completely consistent with this assumption [32].

In conclusion the authors thank D. M. Kaminker for constant interest in this study, and their colleagues in the Measurement Center of the Neutron-Research Laboratory and the reactor staff for assistance in the measurements.

LITERATURE CITED

1. N. Feather, Proceedings of the Second Symposium on the Physics and Chemistry of Fission, Vienna, July, 1969; IAEA, Vienna (1970), p. 83.
2. H. W. Schmitt et al., Phys. Rev. Lett., 9, 427 (1962).
3. M. Asghar et al., Nucl. Phys., A145, 657 (1970).
4. W. D. Loveland, A. W. Fairhall, and J. Halpern, J. Phys. Rev., 163, 1315 (1967); A. V. Drapchinskii et al., At. Énerg., 16, 144 (1964).
5. Z. Fraenkel and S. G. Thompson, Phys. Rev. Lett., 13, 438 (1964).
6. P. Fong, Phys. Rev., 102, 434 (1956).
7. B. T. Geilikman and G. I. Khlebnikov, At. Énerg., 18, 218 (1965).
8. Y. Boneh, Z. Fraenkel, and I. Neberzahl, Phys. Rev., 156, 1305 (1967).
9. V. N. Andreev, V. G. Nedopekin, and V. I. Rogov, Yad. Fiz., 8, 38 (1968).
10. J. Blocki and T. Krogulski, Nucl. Phys., A122, 417 (1968).
11. G. M. Raisbeck and T. D. Thomas, Phys. Rev., 172, 1272 (1968).
12. A. A. Vorob'ev et al., Reprint FTI-215 [in Russian], Leningrad (1969).
13. S. W. Cooper, J. Cerny, and R. S. Gatti, Phys. Rev., 154, 1193 (1967).
14. M. Dakowski et al., Phys. Lett., 25B, 213 (1967).
15. V. N. Andreev, V. G. Nedopekin, and V. I. Rogov, Yad. Fiz., 9, 23 (1969).
16. Y. Gazit, E. Nardi, and S. Katcoff, Phys. Rev., 1C, 2101 (1970).
17. A. A. Vorob'ev et al., At. Énerg., 27, 31 (1969).
18. J. Chwaszczewska et al., Acta Phys. Polon., 34, 173 (1968).
19. L. C. Northcliffe, in: Annual Reviews of Nuclear Science, Vol. 13 (1963), p. 67.
20. A. A. Vorob'ev (Vorobiev) et al., Phys. Lett., 30B, 832 (1969).
21. T. Krogulski et al., Nucl. Phys., A128, 219 (1969).
22. J. Blocki et al., Nucl. Phys., A127, 495 (1969).
23. V. N. Andreev, V. G. Nedopekin, and V. I. Rogov, Yad. Fiz., 9, 23 (1969).
24. E. N. Sloth et al., J. Inorg. Nucl. Chem., 24, 337 (1962).
25. D. L. Horrocks and E. B. White, Nucl. Phys., A151, 65 (1960).
26. A. A. Vorob'ev et al., Preprint FTI-232 [in Russian], Leningrad (1969).
27. A. M. Poskanzer, G. W. Butler, and E. K. Hyde, UCRL-18996 (1970).
28. I. Halpern, Unpublished CERN report (1963).
29. H. W. Schmitt, J. H. Neiler, and E. J. Walter, Phys. Rev., 141, 1146 (1966).
30. N. Feather, Phys. Rev., 170, 1118 (1968).

31. N. Blocki et al., Proceedings of the Second Symposium on the Physics and Chemistry of Fission, Vienna, July, 1969; IAEA, Vienna (1970), p. 115.
32. E. Nardi, Y. Boneh, and Z. Fraenkel, Proceedings of the Second Symposium on the Physics and Chemistry of Fission, Vienna, July, 1969; IAEA, Vienna (1970), p. 143.